Available online at www.sciencedirect.com
ScienceDirect
Journal of Sound and Vibration 300 (2007) 662–675
JOURNAL OF SOUND AND VIBRATION
www.elsevier.com/locate/jsvi

Modelling of constrained thin rubber layer with emphasis on damping

Magnus Alvelid[a,*], Mikael Enelund[b]

[a]Trelleborg Rubore AB, SE-39128 KALMAR, SWEDEN and Applied Mechanics, Chalmers University of Technology, SE-41296 Göteborg, Sweden
[b]Applied Mechanics, Chalmers University of Technology, SE-41296 Göteborg, Sweden

Received 4 October 2005; received in revised form 19 July 2006; accepted 6 August 2006
Available online 27 October 2006

Abstract

An interface finite element for the rubber layer in a steel–rubber–steel sandwich plate is developed. The novel element is based on a series expansion of the displacement field in the thickness direction. This technique makes it possible to achieve a high resolution of the displacement field in the thickness direction without adding more degrees-of-freedom in this direction. A fractional order viscoelastic model is used to describe the constitutive behavior of rubber. In particular, we consider a ''Nitrile'' type rubber and fit the model parameters to experiments. The purpose and the predictive capability of the interface element are investigated by calculating the harmonic response of sandwich plates. The results are then compared with measured responses as well as with responses obtained by a commercial general purpose finite element code and an analytical solution for a sandwich beam equation. Finally, we conclude that the interface element is accurate and efficient in the modelling of constrained rubber layers.

1. Introduction

Noise and vibration is an environmental problem that continuously calls for resources to be handled. For all kinds of vehicles, automobiles, airplanes, ships, etc., the interior and exterior noise and vibrations levels are among the most important design criteria. The combination with other desired properties of the product, such as low weight, drives the development work into significant challenges. In aircrafts and some high end cars, active noise control has been one way to meet the technical demands but at the expense of higher cost. For cars though, it is more common to add passive damping materials to the structure in order to decrease noise and vibration levels. In any case, advanced, effective, general and robust engineering tools are required in order to predict noise and vibrations.

Body structures for, e.g., automotive, space, aeronautical and naval applications are, to a large extent, consisting of thin walled structures and corresponding finite element models are most often built from shell elements. Although modelling with three-dimensional solid elements is becoming more and more common for

*Corresponding author. Tel.: +46 708 698903.
E-mail addresses: magnus.alvelid@telia.com (M. Alvelid), mikael.enelund@chalmers.se (M. Enelund).

0022-460X/$ - see front matter © 2006 Elsevier Ltd. All rights reserved.
doi:10.1016/j.jsv.2006.08.031

thin-walled structures, thanks to the extra-ordinary development of computer hardware capacity during a number of years, engineers will never have unlimited resources in terms of degrees-of-freedom to spend on a finite element model. Therefore, there will always be a trade off between the simplicity in modelling using solid modelling and the extra number of degrees-of-freedom it will cause.

It is found from a continuous cooperation over several years with the large and well known car manufacturers, that today, within the automotive industry, shell modelling is the totally dominating finite element modelling (FEM) technique on the car ''body-in-white'' level. Thus, any investigation on the effect of ''applied damping material'' (ADM) to the structure will have to cope with the fact that the existing base structure FE model is made up of shell elements. Also, almost the whole community of car manufacturers reports large difficulties in how to accurately enough model viscoelastic materials, and to get correlation with measurements. An easy-to-use and accurate material model which can be communicated using only a few parameters is therefore key to an improvement within this field.

A generally accepted fact is that applied damping material in the form of ''constrained layer damping'' (CLD) is very efficient in terms of reducing vibration energy. The technical principle is that of a high loss factor viscoelastic layer (e.g. rubber) attached to the base structure and constrained on its other side by a stiff layer (e.g. metal). Thus, when the base structure vibrates in bending the viscoelastic layer will be subjected to large shear deformation, resulting in conversion of kinetic energy into heat. Given an existing finite element mesh for the base structure, the constraining layer will most certainly be modelled with shell elements. An efficient way of modelling the viscoelastic layer in between so as to couple these two shells together is therefore needed.

There are several perspectives on the field of constrained layer damping. From the 1950s and onwards, the work produced by Kerwin [1], Yin et al. [2], DiTaranto and McGraw [3], Mead and Markus [4] and Yan and Dowell [5] have layed the foundation for aftercoming researchers. During the late 1970s, FEM was introduced by Lu et al. [6] as a general method for solving problems of sandwich plates with general boundary conditions, by using the commercial finite element code NASTRAN and was followed up in Ref. [7] with the application on circular structures. A few years later, Johnson and Kienholz [8] demonstrated how the modal strain energy method could be applied on a CLD problem by introducing correction factors to the modal loss factors found from undamped mode shapes and material loss factors, and thereby increase accuracy. Especially for three-dimensional problems with plate or shell type structures, these results catalyzed the research in this direction because of the new tool they offered for verifying and validating new material models, simulation techniques, etc., where closed form solutions or expansions into reasonably simple base functions were difficult to find. The majority of all research within the field of CLD is done on beam structures. The ease of understanding the fundamentals of the problem, demonstrability and a variety of options for verifying the solutions like closed form solutions and series expansions may be some of the reasons for this.

The application of fractional calculus for viscoelastic problems has found its applications even for CLD. Following the introduction of the technique by Bagley and Torvik [9] and further development by Enelund [10] and others, Galucio et al. [11] use fractional calculus in the constitutive model of the core of a sandwich beam element and the solving of a transient problem for a simply supported beam consisting of only the viscoelastic core.

A different way of representing the viscoelastic material behavior was introduced by Golla and Hughes [12] and McTavish and Hughes [13] (GHM) where the shear modulus is represented by a series of damped mini-oscillators. As an application of this, Meunier and Shenoi [14] have demonstrated how a transient and steady-state analysis of a sandwich panel can be carried out using the GHM method to represent the material modulus of the viscoelastic core with fiber reinforced plastics in the facing materials.

A key issue in all these studies is an accurate determination or estimation of the material parameters, given the chosen constitutive model. In a recent article, Lakes [15] gives a review of the basics in the viscoelastic material behavior and the corresponding appropriate measurement technique, as well as some examples of instrumentation that can be used. In linear viscoelasticity, and especially for the dynamics of rubber like materials, the two main data of interest are the storage and loss part of the shear modulus. The material parameters depend heavily on frequency and temperature. Nashif et al. [16] outline extensively how tests using cantilever beams can be used for extracting the complex and frequency dependent shear modulus from eigenvalue extraction at different temperatures, comparing a base (undamped) structure with a system built up

from different layers of material. This has resulted in the standard procedure described in ASTM 756-98 and is the procedure used here.

Most of the work performed within CLD are dealing with linear problems. Daya et al. [17], however, demonstrate how geometrical nonlinearities arising from second-order terms in the strain–displacement relation can be taken account for in the analysis, and points out that depending on the vibration amplitudes, the system can go nonlinear because of the effects of the axial stresses in the face layers. For the problems considered vibration levels are small and linearity is a reasonably assumption.

Different kinds of expansions of the displacement field into suitable sets of base functions, depending on the character of the boundary value problem, are very common tools in order to get a formulation that can be solved for analytically, or in order to get a reduced number of degrees-of-freedom when the technique is used within the FEM domain. A variant of this is the p-element method where the order of the interpolating shape functions of the displacement field is increased until the convergence criteria is reached. Leung et al. [18] use trigonometric, additional and internal shape functions of varying order in two-dimensional elements, and show that convergence can be reached much faster than with conventional h-element technique for a viscoelastic vibration problem, thus reducing computation time. Another example is presented by Zhang et al. [19] where orthogonal functions are combined with polynomials in a FE context and thereby faster convergence is reached.

During recent years, the interest in different kinds of optimization problems have increased considerably, resulting in a large number of studies in the field. One of the most often cited references is Nakra [20] who investigated various locations for additive damping on a plates and beams. However, as is pointed out by Stanway et al. [21], passive CLD has its drawback in that for lower frequencies, a relatively small portion of the viscoelastic material will be engaged in shear and therefore the transfer of vibrational energy into heat will be limited. As a result of this, ''active constrained layer damping'' (ACLD) has, as of today, become an area of large interest. In this application, an electrical voltage is applied to a piezoelectric material via a control loop, and creates a secondary and superimposed vibration field that can cancel part of the primary vibrations. A large number of studies within this field have been performed the last 3–4 years, the majority of which examines different aspects of a sandwich beam problem with ACLD. Illaire and Kropp [22] make a study of a modified version of Baz's sixth-order differential equation for a sandwich beam, and introduces indices that can be used for determining the efficiency of the different damping mechanisms separately.

Another important aspect of the vibration problem is whether lower vibration levels leads to a better noise emission situation. Kari et al. [23] have in a realistic experiment investigated if the reduced vibration levels leads to correspondingly lower levels in sound intensity in the surrounding air. They found that for the actual study, this was not the case because of the better radiation efficiency of the structure after that the damping layer had been applied. They even found that for a single one third octave band, the sound intensity was higher than without the treatment. But over the whole frequency range, the reduction in sound intensity was significant by using the treatment.

It has been found that although there has been much research done within this field, there is a general lack of efficient analysis tools that can be used in order to investigate the effect of adding constrained layer damping to an existing finite element model consisting of shell elements. A significant contribution to improve the current situation would be the invention of a general, accurate and easy-to-use interface finite element that can directly couple together the base structure shell elements, the viscoelastic layer and the constraining layer shell elements. A significant advantage of this approach, compared to the approach where specialized finite elements for the whole sandwich structure is developed, is that the connecting shells can be modelled using any shell elements. The fractional viscoelastic model will be used to describe the constitutive behavior of the rubber. This model is chosen because of its ability to accurately represent the behavior of the rubber material over a very large frequency band using only a few parameters, as low as four in the uniaxial case. The model parameters will be fit to experimental data over a broad frequency range. Further, in the thickness direction, the finite element discretization will be based on a power series development so that a general displacement field can be represented without adding nodes. The interface element will be applied on problems with direct industrial relevance. In particular, we will consider a sandwich structure consisting of a thin rubber layer and two steel plates. The harmonic response of two different structures will be calculated and compared with experiments and analytical solutions.

2. Constitutive modelling

A common rubber type used in the present applications is based on "Nitrile" rubber (acryl-nitrile-butadien). The rubber quality used in this study has about 35% content of carbon black. Vulcanization is achieved using a substance that emits sulfide and thereby creates monosulfide cross-links. The rubber adheres to the steel plates by a process involving high pressures at elevated temperatures where the steel plates have been pretreated with a very thin adhesive.

2.1. Fractional order viscoelasticity

The nitrile rubber is found to be viscoelastic and nearly incompressible. The viscoelastic behavior is obvious from the measured frequency behavior of the dynamic shear modulus see, Fig. 1. Further, the Poisson ratio is measured with high precision and found to be $v = 0.4993$. In the intended application, the strains are assumed to be small and a linear constitutive model will suffice. The thin rubber layer is bonded to metal plates that are very good heat conductors and isothermal conditions may be assumed for the rubber layer. The constitutive behavior of the rubber material (under isothermal and isotropic conditions) is then characterized by a standard linear viscoelastic model. However, by using a classical viscoelastic model that is based on first-order rate laws for the internal variables, a large number of internal variables and, consequently, a large number of model parameters are required to describe the viscoelastic behavior. By using fractional order operators in the constitutive equations the number of parameters required is significantly reduced. The fractional order linear viscoelastic model has successfully been fit to experimental data over a broad frequency range for several polymers using only four parameters (two "elastic" constants, one relaxation constant and the non-dimensional fractional order of differentiation) in the uniaxial case, see, e.g., Refs. [9,24]. Now consider the simplest fractional order viscoelastic model (FoV) that can reproduce solid behavior with instantaneous and long time elastic responses. The constitutive equation for the shear stress τ can be written as two coupled equations

$$\begin{aligned} \tau(t) &= G_0\gamma(t) - (G_0 - G_\infty)\gamma^{\mathrm{v}} \\ \mathrm{D}^\alpha\gamma^{\mathrm{v}} + \frac{1}{\tau_*^\alpha}\gamma^{\mathrm{v}} &= \frac{1}{\tau_*^\alpha}\gamma, \quad \gamma^{\mathrm{v}}(0) = 0, \end{aligned} \tag{1}$$

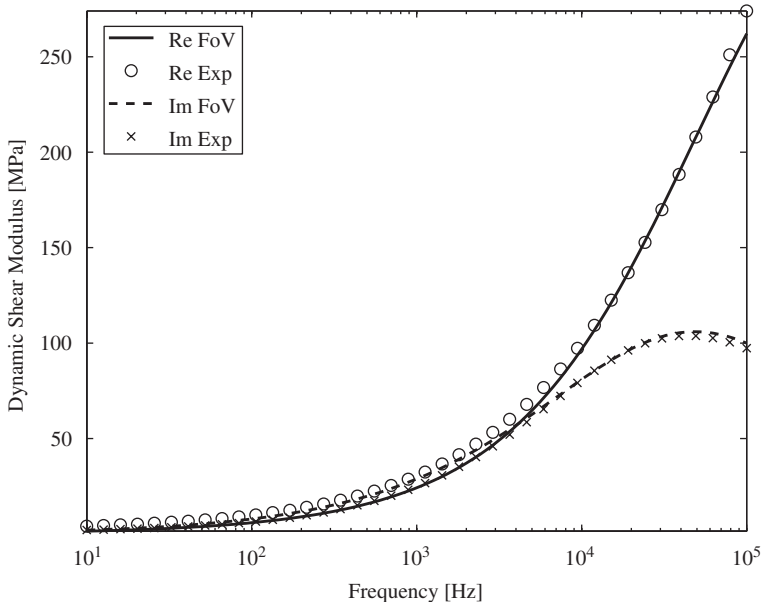

Fig. 1. Parameter fit of the fractional order viscoelastic model (FoV) to experimental data (Exp) for the nitrile rubber. Solid line represents curve-fitted real part and circle-marks represent real part experimental data while dashed line represents curve fitted imaginary part and x-marks represent imaginary part experimental data.

where γ is the (macroscopic) shear while γ^{v} is an internal variable of shear type representing a distribution of irreversible microstructural processes in the material, $G_0 > 0$ and $G_\infty > 0$ are elastic constants which can be identified as instantaneous and long time shear modulus, respectively, t_* is the relaxation constant and D^α is the fractional derivative operator of order $\alpha \in (0, 1)$

$$\mathrm{D}^\alpha y(t) = \frac{1}{\Gamma(1-\alpha)} \frac{\mathrm{d}}{\mathrm{d}t} \left[\int_0^t \frac{y(s)}{(t-s)^\alpha} \mathrm{d}s \right]. \tag{2}$$

Note that the fractional differential operator is not a local operator, i.e., the derivative is not only dependent of the value at the specific point in time but the value of the function on the whole interval. The Fourier transform of the fractional derivative operator can be written as

$$F[\mathrm{D}^\alpha y(t)](\omega) = (\mathrm{i}\omega)^\alpha F[y(t)](\omega). \tag{3}$$

By applying a Fourier transform to the constitutive equations in Eq. (1), the internal variable can be eliminated and the constitutive equations can be written as a single equation

$$\tau(\omega) = G^*(\omega)\gamma(\omega) \quad \text{with } G^*(\omega) = G_0 - \frac{G_0 - G_\infty}{1 + (t_* \mathrm{i}\omega)^\alpha}, \tag{4}$$

where G^* is denoted the dynamic shear modulus.

2.2. Parameter fit

The constitutive parameters in Eq. (4) are estimated by a least-square fit to experimental data of the dynamic shear modulus. The real and imaginary part of the dynamic shear modulus as a function of temperature and frequency was first experimentally obtained using a sandwich cantilever specimen (see Fig. 2) and the procedure in ASTM E756-98 (see, e.g., the textbook [16]). A non-contact electromagnetic excitation is placed at the free end of the specimen. A piezo-electric crystal response transducer picks up the signal close to the clamping. The temperature is then varied in steps of 10 °C, from −30 to 180 °C. After thermal equilibrium is reached, the dynamic tests are performed. Typical soak time is 30 min. For each temperature, the eigenfrequencies for the vibration modes are measured together with the half-power bandwidth. The first mode is excluded. Usually, mode two to mode seven are extracted and the dynamic shear modulus G^* is calculated using the procedure in the standard. The following parameter values were identified

$$G_0 = 414\,\mathrm{MPa},\ G_\infty = 4.0\,\mathrm{MPa}, \quad t_* = 3.31 \cdot 10^{-6}\,\mathrm{s}, \quad \text{and} \quad \alpha = 0.60.$$

Fig. 1 shows the parameter fit of the fractional order model of viscoelasticity to the dynamic shear modulus. Obviously by carrying out the parameter fit in a more narrow frequency band we would have obtained a closer fit in the selected frequency band. However, it is essential for the model to be able to capture the characteristic

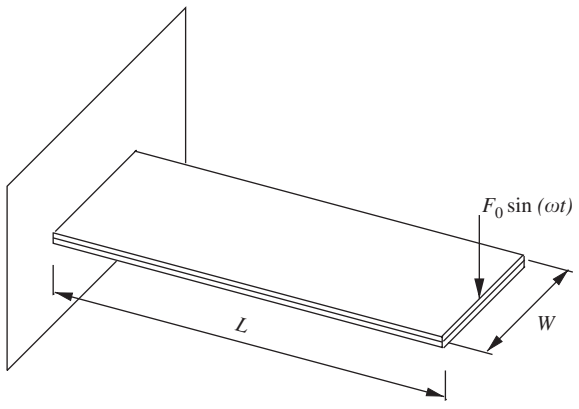

Fig. 2. Sandwich specimen including loading case. $W = 25.4$ mm and $L = 150$ mm.

rubber behavior over a broad frequency range. This is motivated by the fact that the operating temperature in vehicle applications may vary from −30 to 120 °C. In this perspective, the room temperature behavior at 10^8 Hz is important in order to reflect the character at low temperatures based on the frequency–temperature superposition principle. At low temperatures the transition from weak to stiff behavior is shifted towards lower frequencies, see, e.g., Ref. [16].

3. Modelling of thin rubber layer

A typical product configuration is shown in Fig. 3. The product is composed of two steel sheets and one rubber sheet in between. The current case has dimensions $h_1 = h_2 = 0.5$ mm and $t = 0.1$ mm, which gives a dimension ratio of 5:1 for the sandwich construction. This is quite typical for the products on the market, but ratios up to 10:1 are also common. There are also other configurations supplied to the market, with two or more rubber layers, with the relation $n = m + 1$, where m and n are the number of rubber layers and steel layers, respectively. Given the typical dimension ratios, this suggests that the rubber layers can be considered as thin compared to the metal sheets.

In this study, galvanized steel is used in the metal sheets. The material damping in the metal sheets is neglected. The equation of motion for the rubber material under steady-state harmonic conditions (the general time dependence $e^{i\omega t}$ is suppressed) is (in tensor indicial notation)

$$(\lambda^* + \mu^*)\partial^2 u_j/\partial x_j \partial x_i + \mu^* \partial^2 u_i/\partial x_j \partial x_j + \omega^2 \rho u_i = 0, \tag{5}$$

where λ^* and μ^* are the dynamic Lamé constants, ρ is the density of the material and u_i are the displacement amplitudes. The dynamic Lamé constants are related to the dynamic shear modulus through

$$\mu^* = G^*, \quad \lambda^* = \frac{2\mu^* v}{1 - 2v}, \tag{6}$$

where we, for convenience, assume the same viscoelastic behavior in shear and volumetric deformations. The consequence is that Poisson's ratio does not vary with frequency. This can be justified since the material is nearly incompressible meaning that the material deformation in bulk is negligible compared to shear deformations.

Using a similar procedure as in Ref. [25], the field of displacement amplitudes $u_i(x, y, z)$ for the rubber is expanded into a power series in the thickness direction (z) as

$$u_i(x, y, z) = u_{i0}(x, y) + z u_{i1}(x, y) + z^2 u_{i2}(x, y) + \ldots, \tag{7}$$

where in this case both symmetric and anti-symmetric terms are included. The boundary conditions on the top and the bottom surface of the rubber layer are, respectively,

$$u_i(x, y, t/2) = v_{1i}(x, y, -h_1/2), \tag{8}$$

$$u_i(x, y, -t/2) = v_{2i}(x, y, h_2/2), \tag{9}$$

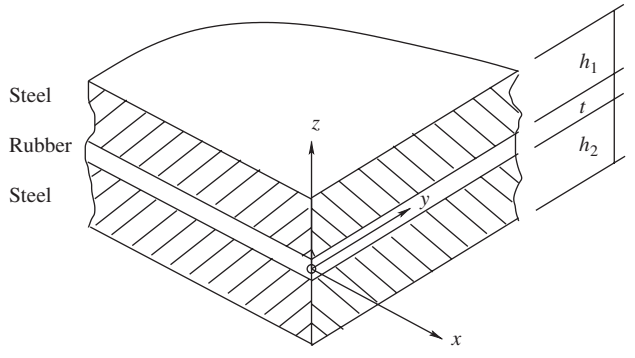

Fig. 3. Product configuration.

where $v_{1i}(x,y,-h_1/2)$ is the displacement amplitude of the bottom surface of shell 1 and $v_{2i}(x,y,h_2/2)$ is the displacement amplitude of the top surface of shell 2 (cf . Fig. 3). Input of the series expansion Eq. (7) into the equation of motion Eq. (5) yields the following recursion formulas for the series expansion coefficients (here $u=u_1$, $v=u_2$ and $w=u_3$):

$$(\lambda^*+2\mu^*)\left(\frac{\partial^2 u_k}{\partial x^2}+\mu^*\frac{\partial^2 u_k}{\partial y^2}\right)+\rho\omega^2 u_k+(\lambda^*+\mu^*)\frac{\partial^2 v_k}{\partial x\partial y}+(k+1)(\lambda^*+\mu^*)\frac{\partial w_{k+1}}{\partial x}+(k+1)(k+2)\mu^* u_{k+2}=0, k=0,1,2,\ldots, \tag{10}$$

$$\lambda^*+2\mu^*)\left(\frac{\partial^2 v_k}{\partial y^2}+\mu^*\frac{\partial^2 v_k}{\partial x^2}\right)+\rho\omega^2 v_k+(\lambda^*+\mu^*)\frac{\partial^2 u_k}{\partial x\partial y}+(k+1)(\lambda^*+\mu^*)\frac{\partial w_{k+1}}{\partial y}+(k+1)(k+2)\mu^* v_{k+2}=0, k=0,1,2,\ldots, \tag{11}$$

$$\mu^*\left(\frac{\partial^2 w_k}{\partial x^2}+\frac{\partial^2 w_k}{\partial y^2}\right)+\rho\omega^2 w_k+(k+1)(\lambda^*+\mu^*)\left(\frac{\partial u_{k+1}}{\partial x}+\frac{\partial v_{k+1}}{\partial y}\right)+(k+1)(k+2)(\lambda^*+2\mu^*)w_{k+2}=0,\quad k=0,1,2,\ldots\ . \tag{12}$$

It can be shown that all higher order terms (including order $k=2$ and above) can be expressed as linear combinations of u_{i0} and u_{i1}. We thus have six unknown functions, $u_{i0}(x,y)$ and $u_{i1}(x,y)$ to solve for. This is done using a FE discretization. The formulation is general and higher resolution in the thickness direction can be achieved by increasing the number of nodes in the *in-plane directions* and, thus, capture higher order spatial derivatives.

4. Finite element formulation

The rubber layer is connected to steel sheets on both sides. The steel sheets are modelled using shell elements. We are interested in a direct connection between the shell element degrees-of-freedom and the rubber displacements, resulting in that the bandwidth is kept to a minimum, see, e.g., Ref. [26]. Therefore, we use a five degree-of-freedom (dof) per node formulation for the interface element. The coefficients in Eq. (7) are approximated in terms of interpolations from the nodal degrees-of-freedom. We get the following expressions for u_{i0} and u_{i1}:

$$\begin{Bmatrix} u_{i0}(x,y) \\ u_{i1}(x,y) \end{Bmatrix} = \mathbf{H}\{\mathbf{d}\}. \tag{13}$$

In order to reach compatibility between the covering faces and the viscoelastic core, the same interpolation functions are used for the series expansion coefficients as for the shell elements. The total expression above is built in the following way: first we discretize the coefficient functions using generalized coordinates and interpolating functions, where the generalized coordinates represent the actual value of the coefficients at the in-plane position of the nodal points as

$$\begin{Bmatrix} u_{i0}(x,y) \\ u_{i1}(x,y) \end{Bmatrix} = \mathbf{N}\{\mathbf{u_{ig}}\}. \tag{14}$$

Secondly, we conclude that because kinematic equality between the displacement field of the core and the displacement field of the cover sheets must hold for all in-plane positions at the interfaces, it will also hold at the nodal positions. This results in a system of equations where the generalized coordinates can be solved for, given the actual displacement values on the interfaces like

$$\mathbf{T}_1\{\mathbf{u}_{ig}\} = \{\mathbf{d}_i\}, \tag{15}$$

where $\{\mathbf{d}_i\}$ is the vector of displacements on the interfaces. From the shell geometry, $\{\mathbf{d}_i\}$ is readily available from the nodal displacements with the relation

$$\{\mathbf{d}_i\} = \mathbf{T}_2\{\mathbf{d}\}. \tag{16}$$

Finally, we can expand Eq. (13) into

$$\begin{Bmatrix} u_{i0}(x,y) \\ u_{i1}(x,y) \end{Bmatrix} = \mathbf{N}\mathbf{T}_1^{-1}\mathbf{T}_2\{\mathbf{d}\}. \tag{17}$$

4.1. 8 node linear interface element

An eight-node three-dimensional interface element using an isoparametric formulation is now developed and investigated. In this case, we truncate the series expansion from the second-order term. This makes it possible to directly identify the expressions for the coefficients and a physical interpretation is also clear. We get

$$u_{i0} = (1/2)\sum_j N_j d_j, \tag{18}$$

$$u_{i1} = (1/t)\left(\sum_k N_k d_k - \sum_m N_m d_m\right), \tag{19}$$

where the summation in u_{i0} spans over all nodes in the element while the first summation in u_{i1} spans over the nodes at $z = t/2$ and the second summation spans over the nodes at $z = -t/2$, N_j, N_k, and N_m are the interpolation functions and d_j, d_k, and d_m are the nodal values. In this case, u_{i0} represents a rigid body translation of the cross-section at the actual position in the local xy-plane, whereas u_{i1} is the linear part of the series expansion of the displacement field with respect to the local z-direction which corresponds to rotations of the cross-section around the local x- and y-axis and tension/contraction of the cross-section in the local z-direction. The element geometry with node numbering and internal coordinate system is shown in Fig. 4.

The displacements u_i in the continuum part of the element are interpolated from the nodal degrees-of-freedom (using matrix notation)

$$\{\mathbf{u}\} = \mathbf{N}\{\mathbf{d}\}, \tag{20}$$

where $\mathbf{N}$ is the matrix of elemental interpolation functions (the matrix has dimension 3×40 and as an illustration we present one block out of eight)

$$\mathbf{N} = \begin{pmatrix} & f_i & 0 & 0 & 0 & (\tilde{h}_i/2)f_i & \\ \cdots & 0 & f_i & 0 & -(\tilde{h}_i/2)f_i & 0 & \cdots \\ & 0 & 0 & f_i & 0 & 0 & \end{pmatrix},$$

with

$$f_i = N_i(1/2 - \zeta_i\zeta/2), \quad N_i = \frac{(1+\xi_i\xi)(1+\eta_i\eta)}{4},$$

where $\tilde{h}_i = h_1/2$ for $i = 1,2,3,4$ and $\tilde{h}_i = -(h_2/2)$ for $i = 5,6,7,8$. The vector of elemental strains are given by the relation

$$\{\mathbf{e}\} = \mathbf{B}\{\mathbf{d}\}, \tag{21}$$

where $\mathbf{B}$ is readily found by differentiating $\mathbf{N}$ with respect to the local element coordinates and then identifying the strain terms.

The principal of virtual work may now be applied so as to produce the expression for the dynamic and complex element stiffness matrix as

$$\mathbf{k}_{\mathrm{el}} = \int_{V_{\mathrm{el}}} \mathbf{B}^{\mathrm{T}}\mathbf{E}\mathbf{B}\,\mathrm{d}\mathbf{V}. \tag{22}$$

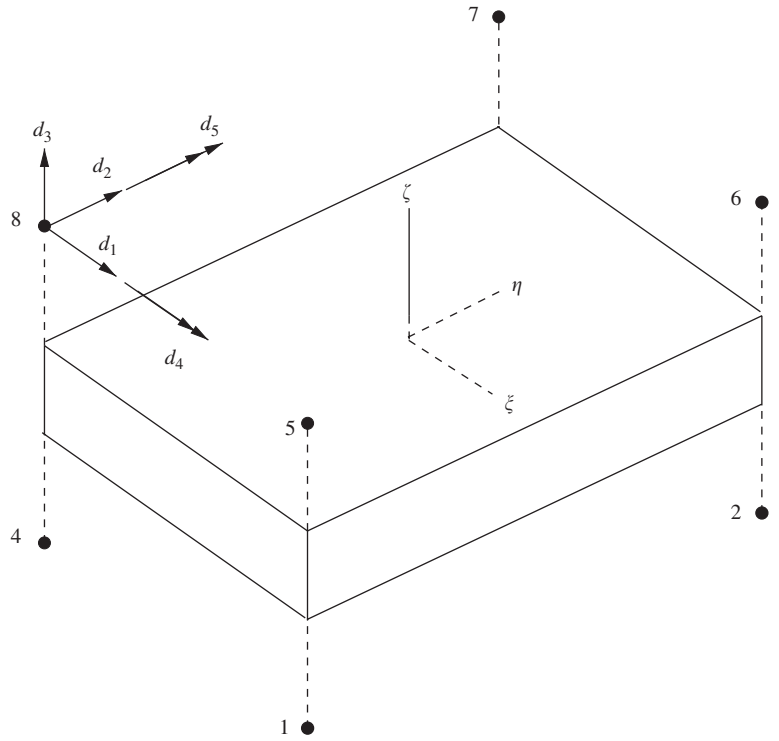

Fig. 4. Interface element geometry with node numbering. A single head arrow indicates a translational nodal degree-of-freedom while a two-head arrow indicates a rotational degree-of-freedom.

Here, **E** is a complex and frequency dependent constitutive matrix for the viscoelastic core. The damping forces are thus included in the element stiffness matrix. The mass matrix is constructed by lumping the element mass to the nodes. Rotational inertia is not taken account for. The mass introduced to each degree-of-freedom in the element is thus $m/8$ where m is the total weight of the element. The element stiffness matrix is calculated using one integration point, located in the middle of the element. This is enough for a first-order variation of displacements in the thickness direction. Potentially, a selective integration scheme as $2 \times 2 \times 1$ with 2×2 integration points in the $\zeta = 0$ plane could be used but was not investigated at present. The coding of the element and the analyses are made in Matlab.

5. Numerical example

5.1. Sandwich cantilever beam

First we consider the sandwich cantilever specimen used in the ASTM E756-98 measurements (see Section 2.2). The specimen is subjected to a transversal unit harmonic load at the free end of the specimen. The specimen is modelled using the present interface element for the rubber layer together with standard 4 node iso-parametric membrane and thick plate elements in combination for the covering steel layers. 35×5 elements are used in the in-plane directions. As references, we analyze the same specimen using the FE-code ABAQUS and solve the vibrating cantilever sandwich beam equation. In ABAQUS, we use the same discretization in the in-plane directions as for the in-house code. In ABAQUS, the metal sheets are modelled by standard elastic thick shell elements and the rubber layer is modelled by linear (8 node) three-dimensional solid elements using the present viscoelastic behavior. The couplings between the shell elements and the solid elements are handled by kinematic constraints. The sandwich beam differential equation is taken from

Mead [4] as

$$\frac{\partial^6 w}{\partial x^6} - g(1+Y)\frac{\partial^4 w}{\partial x^4} + \frac{m}{D_t}\left(\frac{\partial^2 \ddot{w}}{\partial x^2} - g\ddot{w}\right) = 0, \tag{23}$$

where w is the transverse displacement of the structure and m is the mass per unit length of the sandwich beam. g, D_t and Y are given as

$$g = \frac{G}{t_v}\left(\frac{1}{E_b t_b} + \frac{1}{E_c t_c}\right), \quad D_t = E_b I_b + E_c I_c \quad \text{and} \quad Y = b\frac{d^2}{D_t}\frac{E_b t_b E_c t_c}{E_b t_b + E_c t_c},$$

where G is the complex shear modulus of the viscoelastic layer, E_b and E_c are the elasticity modulus of the top and bottom layer of the sandwich while I_b and I_c are the moments of inertia of the top and bottom layers, t_b, t_v and t_c are the layer thicknesses, d is the distance between the neutral lines of the top and bottom layers and b is the width of the beam. For the solution with boundary conditions corresponding to the present example, see Mead [4].

Fig. 5 displays the direct frequency response function using the in-house code with the interface element, analytical solution and ABAQUS. From Fig. 5 we observe that the methods give almost identical results although different element formulations and solutions are used. This verifies the accuracy of our approach. The peak value frequencies from in-house code, ABAQUS and measurements are presented in Fig. 6 and the agreement is satisfactory. Note that the present approach is more efficient than ABAQUS because we do not need to include solid elements and impose kinematic constraints to connect the solid elements to the covering shell elements.

5.2. Free–free sandwich plate

Secondly, we consider the direct frequency response of a 188 × 188 mm square sandwich plate of the same product configuration as in the previous example. The plate is attached to the ground through a nylon string simulating free–free boundary conditions. The test specimen is placed in the test lab several hours before the test is performed to ensure a stable temperature of the material. The temperature in the air surrounding the test set up was measured to 20 °C. The experimental set up is shown in Fig. 7. The excitation is done using an

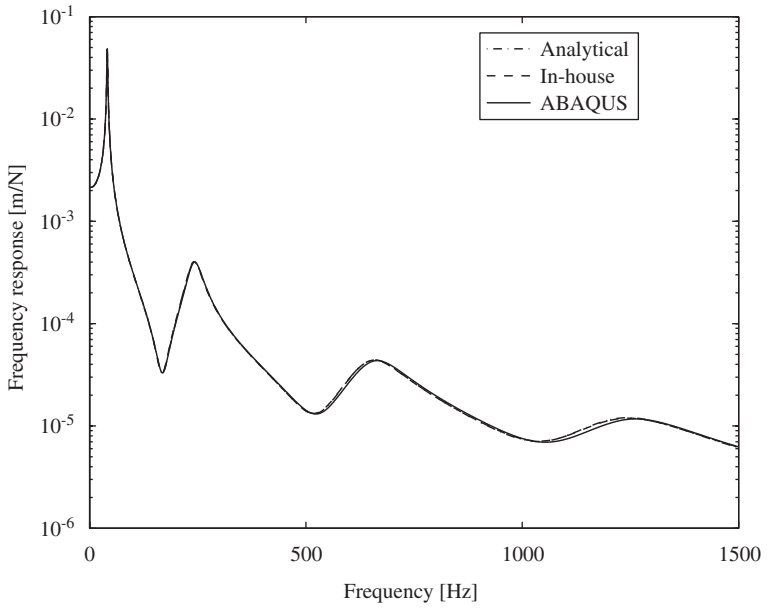

Fig. 5. Calculated direct frequency response (displacement amplitude response to a harmonic unit point load) using the in-house code with the interface element (dashed line), ABAQUS (solid line) and analytic solution to sandwich beam equation (dashdotted line).

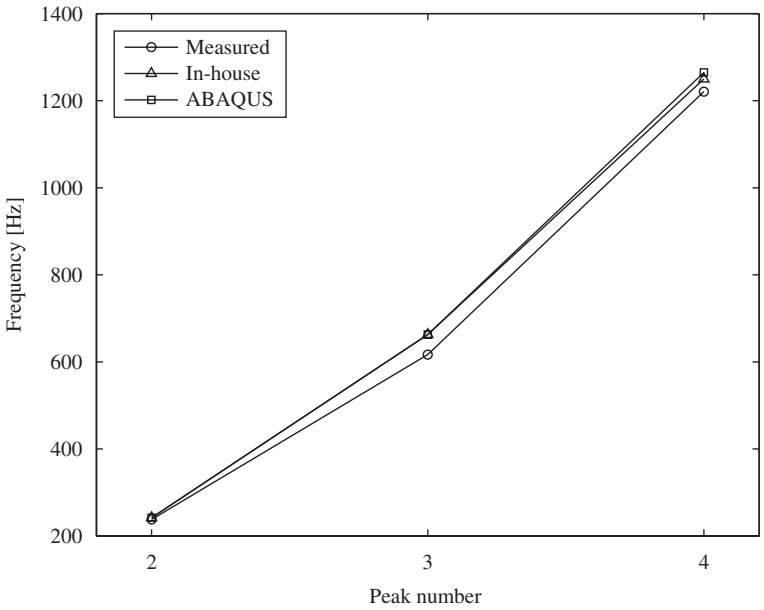

Fig. 6. Peak value frequencies of the frequency response function for the cantilever specimen. Calculated results using in-house code (triangle marks) and ABAQUS (square marks) together with measured frequencies (circle marks).

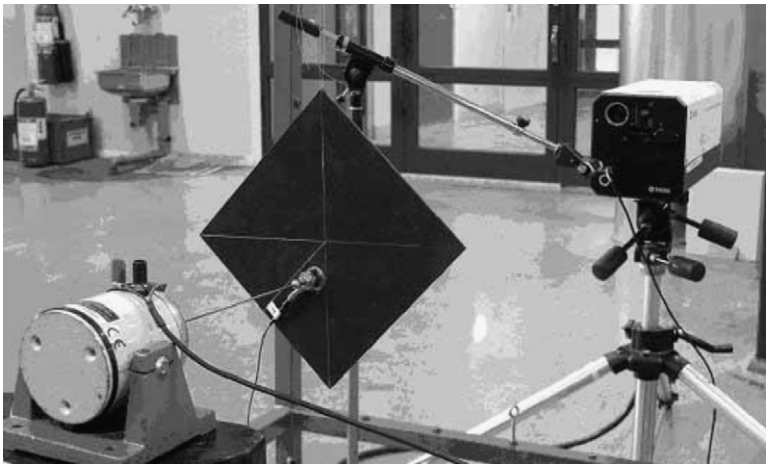

Fig. 7. Experimental set up for frequency response function measurements.

electromagnetic shaker of the type "Wilcoxon F3". The force on the plate is picked up using a force transducer of the type "PCB 352C68 SN 18717". The force transducer is placed between the end of the stinger from the shaker and the plate, so as to correctly measure the input force on the plate. The response amplitude is measured by laser equipment of the type "Polytec PSV 300 scanning laser vibrometer". Generally, coherence and repeatability were very high during the measurements.

The FEM model of the sandwich structure is built up by 13×13 elements in the in-plane directions. This is enough in order to capture the shape of the eigenmodes in the frequency range under study. The highest eigenmode occurring in the frequency band studied in this example is a 2/1 mode, which means that two nodal lines will occur along one of the in-plane directions during the deformation of the plate. Hence, 10 nodes would be sufficient to get a good spatial resolution.

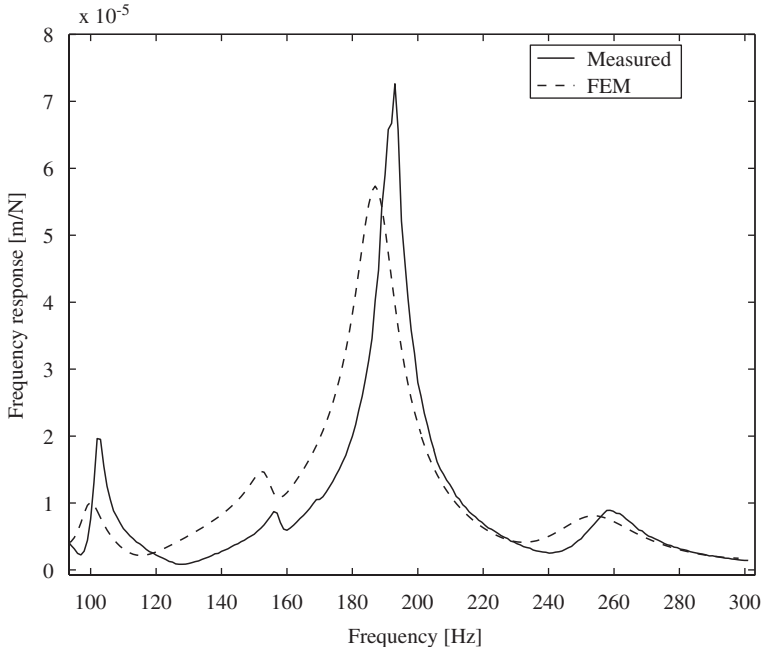

Fig. 8. Measured and calculated direct frequency response of a squared sandwich plate. Solid line represents measured results while dashed line represents calculated results using in-house finite element code.

Fig. 8 presents measured and calculated direct frequency response function of the sandwich plate. The agreement is within 10% which we consider satisfactorily. There are frequency shifts between measured and calculated eigenfrequencies in the figure. By analyzing the dependence of the eigenfrequencies with different parameters in the FEM model, it was found that the eigenfrequencies are very sensitive to variations in steel thickness and to variations in thickness of the sandwich material. Given that the input steel thickness in the FEM model is the nominal value from the steel manufacturer, the major contribution to the frequency shift is believed to originate from dimension variations from the nominal values. If the sandwich material manufacturing process is well controlled, thickness variations of the steel from batch to batch will cause the rubber thickness to vary in accordance. It is found from analyses on sandwich plates with the present rubber material properties, that a small decrease of the steel plate thicknesses at constant sandwich thickness will in fact increase the relationship between stiffness and mass for the sandwich plate and shift the eigenfrequencies upwards. Similarly, an increase in sandwich plate thickness will make the sandwich plate significantly stiffer. On the other hand, a relatively large increase of the rubber storage modulus, up to a 25% increase, did only affect the calculated eigenfrequencies marginally. The measured displacement amplitude is picked up at a point that is a few millimeters away from the node point at which the displacement amplitude is calculated. The sensitivity to this in terms of the response level is different from mode to mode. Over all though, the calculated results are in close agreement with measurements.

6. Discussion and conclusion

A novel interface finite element for the modelling of viscoelastic layers in the application of constrained layer damping has been developed. The element has been verified against measurements and an analytical solution in the case of a beam structure. The present interface element directly couples two layers modelled with shell elements to a viscoelastic layer in between and does not require any extra node definitions. The choice of five degrees-of-freedom per node enables a direct coupling to the shell nodes, and also gives the possibility to couple the shell node rotations correctly via the viscoelastic layer. By this method, node-to-node constraint definitions are not necessary, which considerably reduces engineering cost. Moreover, bandwidth

increase is kept to a minimum which reduces computing cost compared with if multi-point-constraints are used.

The FoV material model is chosen for the interface material. The benefit of this is that the viscoelastic shear behavior can be accurately represented by using only four parameters over a very broad frequency range. Thus, communication of material data parameters within the engineering community is much approved and simplified, and work related to measuring such data can be reduced to standard procedures if the shift functions that relates frequency and temperature dependence for the actual rubber is included. Thus, the resulting material description in the element is accurate and compact, and thereby the use of the element will be very easy.

The spatial discretization uses a power series expansion of the displacement field in the thickness direction. We have shown how such an approach can be introduced. The benefit is that for very stiff viscoelastic layers or for thicker layers, displacement variations through the thickness other than the first approximation (which produces a pure shear) can be described. These effects can be taken into account without having to add more nodes in the thickness direction, which further saves computer resources.

Acknowledgements

Mr. Rickard Jonasson at Trelleborg Rubore AB in Kalmar, Sweden, did all the measurements on the experiments performed and this is greatly acknowledged. The compression mode measurements for extracting the Poisson ratio was performed by Mr. Pierre Charin at Trelleborg France.

References

[1] E.M.J. Kerwin, Damping of flexural waves by a constrained viscoelastic layer, *Journal of the Acoustic Society of America* 31 (1959) 952–962.
[2] T.P.J. Yin, T. Kelly, J. Barry, A quantitative evaluation of constrained-layer damping, *Journal of Engineering for Industry* 89 (1967) 773–784.
[3] R.A.J. Ditaranto, J.J. McGraw, Vibratory bending of damped laminated plates, *Journal of Engineering for Industry* 91 (1969) 1081–1090.
[4] D.J. Mead, S. Markus, The forced vibration of a three-layer damped sandwich beam with arbitrary boundary conditions, *Journal of Sound and Vibration* 10 (1969) 163–175.
[5] M.J. Yan, E. Dowell, Governing equations for vibrating constrained-layer damping sandwich plates and beams, *Journal of Applied Mechanics* 39 (1972) 1041–1046.
[6] Y.P. Lu, J.W. Killian, G.C. Everstine, Vibrations of three layered damped sandwich plate composites, *Journal of Sound of Vibration* 64 (1) (1979) 63–71.
[7] Y.P. Lu, G.C. Everstine, More on finite element modeling of damped composite systems, *Journal of Sound of Vibration* 69 (2) (1980) 199–205.
[8] C.D. Johnson, D. Kienholz, Finite element prediction of damping in structures with constrained viscoelastic layers, *AIAA Journal* 20 (9) (1981) 1284–1290.
[9] R.L. Bagley, P.J. Torvik, Fractional calculus—a different approach to the analysis of viscoelastically damped structures, *AIAA Journal* 21 (5) (1983) 741–748.
[10] M. Enelund, B.L. Josefson, Time-domain finite element analysis of viscoelastic structures with fractional derivatives constitutive relations, *AIAA Journal* 35 (1997) 1630–1637.
[11] A.C. Galucio, J.-F. Deu, R. Ohayon, Finite element formulation of viscoelastic sandwich beams using fractional derivative operators, *Computational Mechanics* 33 (2004) 282–291.
[12] D. Golla, P. Hughes, Dynamics of viscoelastic structures—a time domain, finite element formulation, *Journal of Applied Mechanics* 52 (4) (1985) 897–906.
[13] D. McTavish, P. Hughes, Modeling of linear viscoelastic space structures, *Journal of Vibration and Acoustics* 115 (1) (1993) 103–110.
[14] M. Meunier, R.A. Shenoi, Forced response of FRP sandwich panels with viscoelastic materials, *Journal of Sound and Vibration* 263 (2003) 131–151.
[15] R.S. Lakes, Viscoelastic measurement techniques, *Review of Scientific Instruments—American Institute of Physics* 75 (4) (2004) 797–810.
[16] A.D. Nashif, D.I.G. Jones, J.P. Henderson, *Vibration Damping*, Wiley, New York, 1985.
[17] E.M. Daya, L. Azrar, M. Potier-Ferry, An amplitude equation for the nonlinear vibration of viscoelastically damped sandwich beams, *Journal of Sound and Vibration* 271 (2004) 789–813.
[18] A.Y.T. Leung, B. Zhu, J. Zheng, H. Yang, Two-dimensional viscoelastic vibration by analytic Fourier p-elements, *Thin-Walled Structures* 41 (2003) 1159–1170.

[19] Q.J. Zhang, M.G. Sainsbury, The galerkin element method applied to the vibration of rectangular damped sandwich plates, *Computers and Structures* 74 (2000) 717–730.
[20] B.C. Nakra, Vibration control in machines and structures using viscoelastic damping, *Journal of Sound of Vibration* 211 (3) (1998) 449–465.
[21] R. Stanway, J.A. Rongong, N.D. Sims, Active constrained-layer damping: a state-of-the-art review, *Proceedings of the Institution of Mechanical Engineers Part I—Journal of Systems and Control Engineering* 217 (2003) 437–456.
[22] H. Illaire, W. Kropp, Quantification of damping mechanisms of active constrained layer treatments, *Journal of Sound and Vibration* 1 (2004) 1–19.
[23] L. Kari, K. Lindgren, F. Leping, A. Nilsson, Constrained polymer layers to reduce noise: reality or fiction?—an experimental inquiry into their effectiveness, *Polymer Testing* 21 (2002) 949–958.
[24] S.W.J. Welch, R.A.L. Rorrer, J.R.G. Duren, Application of time-based fractional calculus methods to viscoelastic creep and stress relaxation of materials, *Mechanics of Time-Dependent Materials* 3 (3) (1999) 279–303.
[25] A. Boström, G. Johansson, P. Olsson, On the rational derivation of a hierarchy of dynamic equations for a homogeneous, elastic plate, *International Journal of Solids and Structures* 38 (15) (2001) 2487–2501.
[26] R.D. Cook, D.S. Malkus, M.E. Plesha, *Concepts and Applications of Finite Element Analysis*, Wiley, New York, 1989.